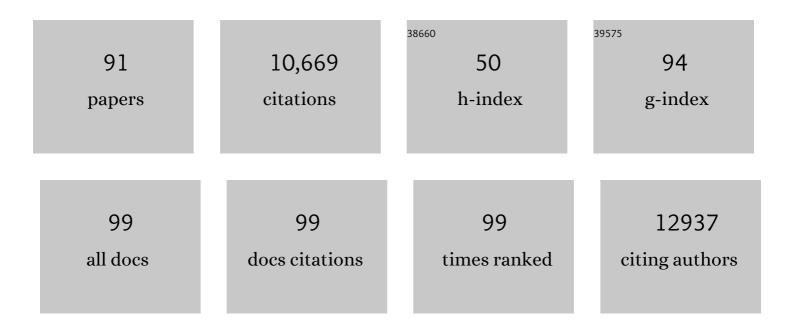
Linfeng Hu

List of Publications by Year in descending order

Source: https://exaly.com/author-pdf/2701333/publications.pdf Version: 2024-02-01



LINEENC HU

#	Article	IF	CITATIONS
1	Simultaneous Incorporation of V and Mn Element into Polyanionic NASICON for High Energyâ€Density and Longâ€Lifespan Znâ€lon Storage. Advanced Energy Materials, 2022, 12, .	10.2	53
2	Realizing Interfacial Electron/Hole Redistribution and Superhydrophilic Surface through Building Heterostructural 2Ânm Co _{0.85} Seâ€NiSe Nanograins for Efficient Overall Water Splittings. Small Methods, 2022, 6, e2200459.	4.6	14
3	Carbonateâ€Hydroxide Induced Metalâ€Organic Framework Transformation Strategy for Honeycombâ€Like NiCoP Nanoplates to Drive Enhanced pHâ€Universal Hydrogen Evolution. Small Methods, 2022, 6, .	4.6	8
4	Vacancies boosting strategy enabling enhanced oxygen evolution activity in a library of novel amorphous selenite electrocatalysts. Applied Catalysis B: Environmental, 2021, 284, 119758.	10.8	55
5	Freeze-drying and hot-pressing strategy to embed two-dimensional Ti0.87O2 monolayers in commercial polypropylene films with enhanced dielectric properties. Journal of Advanced Ceramics, 2021, 10, 368-376.	8.9	3
6	Selenic Acid Etching Assisted Vacancy Engineering for Designing Highly Active Electrocatalysts toward the Oxygen Evolution Reaction. Advanced Materials, 2021, 33, e2007523.	11.1	116
7	Macroporous, Freestanding Birnessite H _{0.08} MnO ₂ ·0.7H ₂ O Nanobelts/Carbon Nanotube Membranes for Wearable Zinc-Ion Batteries with Superior Rate Capability and Cyclability. ACS Applied Energy Materials, 2021, 4, 4138-4149.	2.5	12
8	Bilayered VOPO ₄ â<2H ₂ O Nanosheets with Highâ€Concentration Oxygen Vacancies for Highâ€Performance Aqueous Zincâ€Ion Batteries. Advanced Functional Materials, 2021, 31, 2106816.	7.8	104
9	Spontaneous knitting behavior of 6.7-nm thin (NH4)0.38V2O5 nano- ribbons for binder-free zinc-ion batteries. Energy Storage Materials, 2021, 42, 286-294.	9.5	46
10	Principles of interlayer-spacing regulation of layered vanadium phosphates for superior zinc-ion batteries. Energy and Environmental Science, 2021, 14, 4095-4106.	15.6	121
11	Bilayered VOPO ₄ â<2H ₂ O Nanosheets with Highâ€Concentration Oxygen Vacancies for Highâ€Performance Aqueous Zincâ€Ion Batteries (Adv. Funct. Mater. 45/2021). Advanced Functional Materials, 2021, 31, 2170335.	7.8	3
12	Alleviated Mn ²⁺ dissolution drives long-term cycling stability in ultrafine Mn ₃ O ₄ /PPy core–shell nanodots for zinc-ion batteries. Journal of Materials Chemistry A, 2021, 9, 27380-27389.	5.2	14
13	Ultrathin VSe ₂ Nanosheets with Fast Ion Diffusion and Robust Structural Stability for Rechargeable Zincâ€lon Battery Cathode. Small, 2020, 16, e2000698.	5.2	154
14	A Layered Zn _{0.4} VOPO ₄ ·0.8H ₂ O Cathode for Robust and Stable Zn Ion Storage. ACS Applied Energy Materials, 2020, 3, 3919-3927.	2.5	60
15	Ultrafast Zinc-Ion Diffusion Ability Observed in 6.0-Nanometer Spinel Nanodots. ACS Nano, 2019, 13, 10376-10385.	7.3	124
16	Novel Subâ€5 nm Layered Niobium Phosphate Nanosheets for Highâ€Voltage, Cationâ€Intercalation Typed Electrochemical Energy Storage in Wearable Pseudocapacitors. Advanced Energy Materials, 2019, 9, 1900111.	10.2	57
17	A long-lifespan, flexible zinc-ion secondary battery using a paper-like cathode from single-atomic layer MnO ₂ nanosheets. Nanoscale Advances, 2019, 1, 4365-4372.	2.2	33
18	Thermal transformation of ZnCo1.5(OH)4.5Cl0.5·0.45H2O into hexagonal ZnCo2O4 nanosheets for high-performance secondary ion batteries. Journal of Alloys and Compounds, 2019, 783, 455-459.	2.8	5

LINFENG HU

#	Article	IF	CITATIONS
19	Cu 0.33 Co 0.67 S 2 Hexagonal Sheets with 2D Hierarchical Structures for Highâ€Rate and Longâ€Term Lithium Storage. ChemNanoMat, 2019, 5, 531-538.	1.5	3
20	<i>In Situ</i> Growth of Layered Bimetallic ZnCo Hydroxide Nanosheets for High-Performance All-Solid-State Pseudocapacitor. ACS Nano, 2018, 12, 2968-2979.	7.3	193
21	Rapid Amorphization in Metastable CoSeO ₃ ·H ₂ O Nanosheets for Ultrafast Lithiation Kinetics. ACS Nano, 2018, 12, 5011-5020.	7.3	53
22	Lower ammoniation activation energy of CoN nanosheets by Mn doping with superior energy storage performance for secondary ion batteries. Nanoscale, 2018, 10, 5581-5590.	2.8	31
23	Epitaxial growth of NiCo2S4/Co9S8@Graphene heterogenous nanocomposites with high-rate lithium storage performance. Journal of Alloys and Compounds, 2018, 747, 926-933.	2.8	14
24	CuGaS ₂ nanoplates: a robust and self-healing anode for Li/Na ion batteries in a wide temperature range of 268–318 K. Journal of Materials Chemistry A, 2018, 6, 1086-1093.	5.2	44
25	Electrocatalytic CO2 Reduction: 2D Assembly of Confined Space toward Enhanced CO2 Electroreduction (Adv. Energy Mater. 25/2018). Advanced Energy Materials, 2018, 8, 1870112.	10.2	1
26	Freestanding CoSeO ₃ ·H ₂ O nanoribbon/carbon nanotube composite paper for 2.4 V high-voltage, flexible, solid-state supercapacitors. Nanoscale, 2018, 10, 12003-12010.	2.8	56
27	2D Assembly of Confined Space toward Enhanced CO ₂ Electroreduction. Advanced Energy Materials, 2018, 8, 1801230.	10.2	49
28	Fractal (Ni <i>_x</i> Co _{1â^'} <i>_x</i>) ₉ Se ₈ Nanodendrite Arrays with Highly Exposed () Surface for Wearable, Allâ€Solidâ€State Supercapacitor. Advanced Energy Materials, 2018, 8, 1801392.	10.2	183
29	<i>In situ</i> growth of (NH ₄) ₂ V ₁₀ O ₂₅ ·8H ₂ O urchin-like hierarchical arrays as superior electrodes for all-solid-state supercapacitors. Journal of Materials Chemistry A, 2018, 6, 16308-16315.	5.2	38
30	Forming free and ultralow-power erase operation in atomically crystal TiO ₂ resistive switching. 2D Materials, 2017, 4, 025012.	2.0	14
31	Superior Adsorption and Regenerable Dye Adsorbent Based on Flower-Like Molybdenum Disulfide Nanostructure. Scientific Reports, 2017, 7, 43599.	1.6	118
32	Solutionâ€Growth Strategy for Largeâ€Scale "CuGaO ₂ Nanoplate/ZnS Microsphere― Heterostructure Arrays with Enhanced UV Adsorption and Optoelectronic Properties. Advanced Functional Materials, 2017, 27, 1701066.	7.8	27
33	Pseudocapacitance-tuned high-rate and long-term cyclability of NiCo ₂ S ₄ hexagonal nanosheets prepared by vapor transformation for lithium storage. Journal of Materials Chemistry A, 2017, 5, 9022-9031.	5.2	87
34	Fabrication of novel lamellar alternating nitrogen-doped microporous carbon nanofilm/MoS ₂ composites with high electrochemical properties. Journal of Materials Chemistry A, 2017, 5, 22726-22734.	5.2	12
35	Charge Transfer in Ultrafine LDH Nanosheets/Graphene Interface with Superior Capacitive Energy Storage Performance. ACS Applied Materials & Interfaces, 2017, 9, 37645-37654.	4.0	134
36	Novel Ω‣haped Core–Shell Photodetector with High Ultraviolet Selectivity and Enhanced Responsivity. Advanced Functional Materials, 2017, 27, 1704477.	7.8	29

Linfeng Hu

#	Article	IF	CITATIONS
37	Asymmetric Supercapacitors: Preparation of MnCo ₂ O ₄ @Ni(OH) ₂ Core–Shell Flowers for Asymmetric Supercapacitor Materials with Ultrahigh Specific Capacitance (Adv. Funct. Mater. 23/2016). Advanced Functional Materials, 2016, 26, 4038-4038.	7.8	9
38	Preparation of MnCo ₂ O ₄ @Ni(OH) ₂ Core–Shell Flowers for Asymmetric Supercapacitor Materials with Ultrahigh Specific Capacitance. Advanced Functional Materials, 2016, 26, 4085-4093.	7.8	517
39	Study on electrical defects level in single layer two-dimensional Ta ₂ O ₅ . Chinese Physics B, 2016, 25, 047304.	0.7	4
40	Bottom-up Approach Design, Band Structure, and Lithium Storage Properties of Atomically Thin γ-FeOOH Nanosheets. ACS Applied Materials & Interfaces, 2016, 8, 21334-21342.	4.0	49
41	Selfâ€Templated Synthesis of Ultrathin Nanosheets Constructed TiO ₂ Hollow Spheres with High Electrochemical Properties. Advanced Science, 2016, 3, 1600162.	5.6	28
42	A Novel Sustainable Flour Derived Hierarchical Nitrogenâ€Doped Porous Carbon/Polyaniline Electrode for Advanced Asymmetric Supercapacitors. Advanced Energy Materials, 2016, 6, 1601111.	10.2	303
43	Epitaxial Growth of Latticeâ€Mismatched Core–Shell TiO ₂ @MoS ₂ for Enhanced Lithiumâ€Ion Storage. Small, 2016, 12, 2792-2799.	5.2	71
44	Uniform carbon-coated CdS core–shell nanostructures: synthesis, ultrafast charge carrier dynamics, and photoelectrochemical water splitting. Journal of Materials Chemistry A, 2016, 4, 1078-1086.	5.2	75
45	Nickel Cobaltite Nanostructures for Photoelectric and Catalytic Applications. Small, 2015, 11, 4267-4283.	5.2	127
46	Semiconductors: Controlled Growth from ZnS Nanoparticles to ZnS–CdS Nanoparticle Hybrids with Enhanced Photoactivity (Adv. Funct. Mater. 3/2015). Advanced Functional Materials, 2015, 25, 495-495.	7.8	3
47	One‣tep Selfâ€Assembly Fabrication of High Quality Ni <i>_x</i> Mg _{1<i>â€x</i>} O Bowlâ€Shaped Array Film and Its Enhanced Photocurrent by Mg, ²⁺ Doping. Advanced Functional Materials, 2015, 25, 3256-3263.	7.8	13
48	New concept ultraviolet photodetectors. Materials Today, 2015, 18, 493-502.	8.3	661
49	Cathodoluminescence and Photoconductive Characteristics of Singleâ€Crystal Ternary CdS/CdSe/CdS Biaxial Nanobelts. Small, 2015, 11, 1531-1536.	5.2	14
50	Controlled Growth from ZnS Nanoparticles to ZnS–CdS Nanoparticle Hybrids with Enhanced Photoactivity. Advanced Functional Materials, 2015, 25, 445-454.	7.8	239
51	Nickel–Cobalt Layered Double Hydroxide Nanosheets for Highâ€performance Supercapacitor Electrode Materials. Advanced Functional Materials, 2014, 24, 934-942.	7.8	1,235
52	Energy Harvesting for Nanostructured Selfâ€Powered Photodetectors. Advanced Functional Materials, 2014, 24, 2591-2610.	7.8	217
53	Controllable Fabrication and Photoelectrochemical Property of Multilayer Tantalum Nitride Hollow Sphereâ€Nanofilms. Small, 2014, 10, 3038-3044.	5.2	21
54	Efficient Selfâ€Assembly Synthesis of Uniform CdS Spherical Nanoparticlesâ€Au Nanoparticles Hybrids with Enhanced Photoactivity. Advanced Functional Materials, 2014, 24, 3725-3733.	7.8	211

LINFENG HU

#	Article	IF	CITATIONS
55	New UVâ€A Photodetector Based on Individual Potassium Niobate Nanowires with High Performance. Advanced Optical Materials, 2014, 2, 771-778.	3.6	97
56	Dense Assembly of Gd ₂ O ₃ :0.05X ³⁺ (X = Eu, Tb) Nanorods into Nanoscaled Thin-Films and Their Photoluminescence Properties. ACS Applied Materials & Interfaces, 2014, 6, 1462-1469.	4.0	17
57	Oneâ€Step Hydrothermal Synthesis of 2D Hexagonal Nanoplates of αâ€Fe ₂ O ₃ /Graphene Composites with Enhanced Photocatalytic Activity. Advanced Functional Materials, 2014, 24, 5719-5727.	7.8	331
58	Band Gap Tunable Zn2SnO4 Nanocubes through Thermal Effect and Their Outstanding Ultraviolet Light Photoresponse. Scientific Reports, 2014, 4, 6847.	1.6	60
59	Oneâ€Step Fabrication of Ultrathin Porous Nickel Hydroxideâ€Manganese Dioxide Hybrid Nanosheets for Supercapacitor Electrodes with Excellent Capacitive Performance. Advanced Energy Materials, 2013, 3, 1636-1646.	10.2	342
60	Lowâ€Dimensional Nanostructure Ultraviolet Photodetectors. Advanced Materials, 2013, 25, 5321-5328.	11.1	362
61	Heteroepitaxial Growth of GaP/ZnS Nanocable with Superior Optoelectronic Response. Nano Letters, 2013, 13, 1941-1947.	4.5	67
62	Cathodoluminescence Modulation of ZnS Nanostructures by Morphology, Doping, and Temperature. Advanced Functional Materials, 2013, 23, 3701-3709.	7.8	69
63	Stackingâ€Orderâ€Dependent Optoelectronic Properties of Bilayer Nanofilm Photodetectors Made From Hollow ZnS and ZnO Microspheres. Advanced Materials, 2012, 24, 5872-5877.	11.1	134
64	Oil/water interfacial self-assembly for the organization of hydrophobic NaYF4:Yb, Er nanoplatelets into closely-packed fluorescent nanofilms. Journal of Materials Chemistry, 2012, 22, 944-950.	6.7	15
65	Oil–water interfacial self-assembly of PS/ZnS nanospheres and photoconducting property of corresponding nanofilm. Journal of Materials Chemistry, 2012, 22, 17671.	6.7	10
66	Synthesis and applications of CdSe nano-tetrapods in hybrid photovoltaic devices. Pure and Applied Chemistry, 2012, 84, 2549-2558.	0.9	5
67	Oil–water interfacial self-assembly: a novel strategy for nanofilm and nanodevice fabrication. Chemical Society Reviews, 2012, 41, 1350-1362.	18.7	233
68	Thin SnO ₂ Nanowires with Uniform Diameter as Excellent Field Emitters: A Stability of More Than 2400 Minutes. Advanced Functional Materials, 2012, 22, 1613-1622.	7.8	134
69	General Fabrication of Monolayer SnO ₂ Nanonets for Highâ€Performance Ultraviolet Photodetectors. Advanced Functional Materials, 2012, 22, 1229-1235.	7.8	141
70	Growth and Device Application of CdSe Nanostructures. Advanced Functional Materials, 2012, 22, 1551-1566.	7.8	122
71	An Optimized Ultravioletâ€A Light Photodetector with Wideâ€Range Photoresponse Based on ZnS/ZnO Biaxial Nanobelt. Advanced Materials, 2012, 24, 2305-2309.	11.1	426
72	An Optimized Ultraviolet-A Light Photodetector with Wide-Range Photoresponse Based on ZnS/ZnO Biaxial Nanobelt (Adv. Mater. 17/2012). Advanced Materials, 2012, 24, 2304-2304.	11.1	2

Linfeng Hu

#	Article	IF	CITATIONS
73	Electrical Transport Properties of Large, Individual NiCo ₂ O ₄ Nanoplates. Advanced Functional Materials, 2012, 22, 998-1004.	7.8	297
74	Ultrahigh External Quantum Efficiency from Thin SnO ₂ Nanowire Ultraviolet Photodetectors. Small, 2011, 7, 1012-1017.	5.2	278
75	ZnO Hollow‣phere Nanofilmâ€Based Highâ€Performance and Low ost Photodetector. Small, 2011, 7, 2449-2453.	5.2	209
76	New Ultraviolet Photodetector Based on Individual Nb ₂ O ₅ Nanobelts. Advanced Functional Materials, 2011, 21, 3907-3915.	7.8	285
77	ZnS Nanostructure Arrays: A Developing Material Star. Advanced Materials, 2011, 23, 585-598.	11.1	296
78	Highâ€Performance NiCo ₂ O ₄ Nanofilm Photodetectors Fabricated by an Interfacial Selfâ€Assembly Strategy. Advanced Materials, 2011, 23, 1988-1992.	11.1	181
79	Zinc Sulfide Nanostructure Arrays: ZnS Nanostructure Arrays: A Developing Material Star (Adv.) Tj ETQq1 1 0.784	314 rgBT 11.1	/Oyerlock 10
80	A simple hydrothermal method to synthesise highly pure hexagonal and rhombus α-LiAlO _{2 nanosheets. International Journal of Materials and Product Technology, 2010, 37, 263.}	0.1	2
81	Exfoliation of Layered Europium Hydroxide into Unilamellar Nanosheets. Chemistry - an Asian Journal, 2010, 5, 248-251.	1.7	96
82	One-dimensional inorganic semiconductor nanostructures: A new carrier for nanosensors. Pure and Applied Chemistry, 2010, 82, 2185-2198.	0.9	88
83	Self-Assembled Nanofilm of Monodisperse Cobalt Hydroxide Hexagonal Platelets: Topotactic Conversion into Oxide and Resistive Switching. Chemistry of Materials, 2010, 22, 6341-6346.	3.2	42
84	Synthesis of a Solid Solution Series of Layered Eu _{<i>x</i>} Gd _{1â^'<i>x</i>} (OH) _{2.5} Cl _{0.5} ·0.9H ₂ and Its Transformation into (Eu _{<i>x</i>} Gd _{1â^'<i>x</i>}) ₂ O ₃ with Enhanced	0 1.9	78
85	Photoluminescence Properties. Inorganic Chemistry, 2010, 49, 2960-2968. Oriented Monolayer Film of Gd ₂ 0 ₃ :0.05 Eu Crystallites: Quasiâ€Topotactic Transformation of the Hydroxide Film and Drastic Enhancement of Photoluminescence Properties. Angewandte Chemie - International Edition, 2009, 48, 3846-3849.	7.2	128
86	Template-assisted synthesis of mesoporous LiAlO2 hollow spheres with high surface area. Microporous and Mesoporous Materials, 2008, 113, 41-46.	2.2	6
87	Hydrothermal synthesis of single crystal mesoporous LiAlO2 nanobelts. Materials Letters, 2008, 62, 2039-2042.	1.3	13
88	Oriented films of layered rare-earth hydroxide crystallites self-assembled at the hexane/water interface. Chemical Communications, 2008, , 4897.	2.2	75
89	New composite polymer electrolyte comprising mesoporous lithium aluminate nanosheets and PEO/LiClO4. Journal of Power Sources, 2007, 166, 226-232.	4.0	110
90	Hydrothermal routes to various controllable morphologies of nanostructural lithium aluminate. Materials Research Bulletin, 2007, 42, 1407-1413.	2.7	6

#	Article	IF	CITATIONS
91	Hydrothermal synthesis of high surface area mesoporous lithium aluminate. Materials Letters, 2007, 61, 570-573.	1.3	14